SANC: высокоточное моделирование поляризационных эффектов для процессов на современных коллайдерах

Виталий Ермольчик
от имени группы SANC

ОИЯИ; НИИ ЯП БГУ

Научная сессия
Секция ядерной физики Отделения физических наук
Российской академии наук
02 апреля 2024

CLIC - Compact linear collider

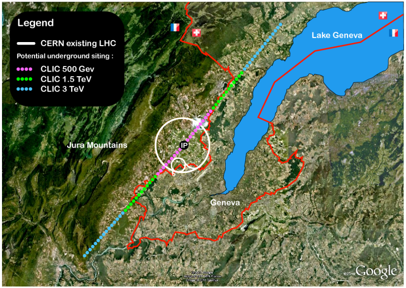

ILC - International linear collider

FCC - Future Circular Collider

CEPC - Circular e^+e^- Collider

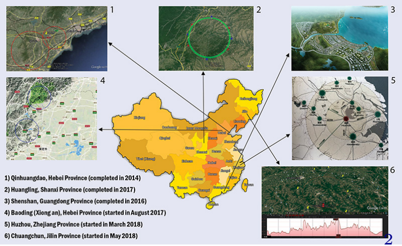

"Chiral Belle"

Beam Polarization Upgrade for SuperKEKB

- Extremely rich and unique high precision electroweak program
- Probe of Dark Sector
- Tau Lepton Magnetic Form factor (τ g-2)
- Improved precision measurements of τ Michel Parameters
- Hadronic studies

Polarized hadron physics

RHIC - Relativistic Heavy Ion Collider

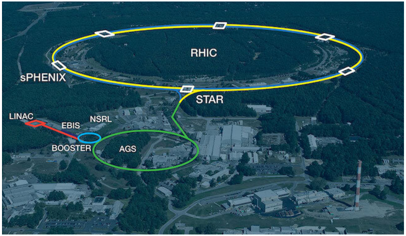

NICA - Nuclotron-based Ion Collider fAcility

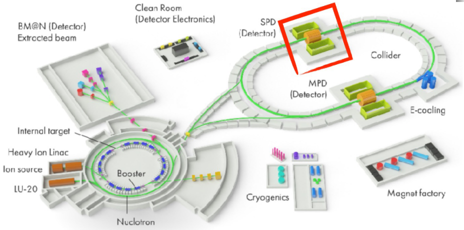

Photon colliders

$e \to \gamma$ conversion through the Compton scattering of laser light on high-energy electrons (I. Ginzburg, G. Kotkin, Phys.Part.Nucl. 52 (2021) 5, 899-912):

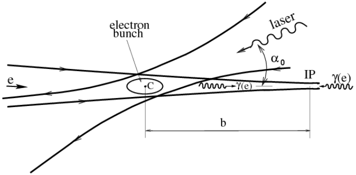

A Planned facility in the IHEP:

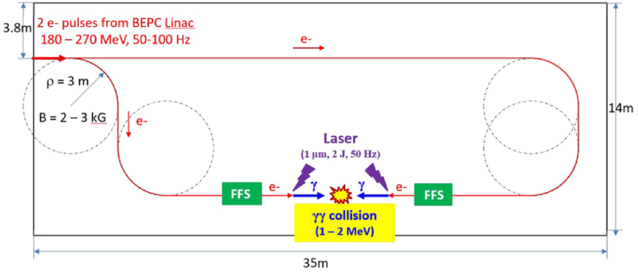

The SANC framework and products family

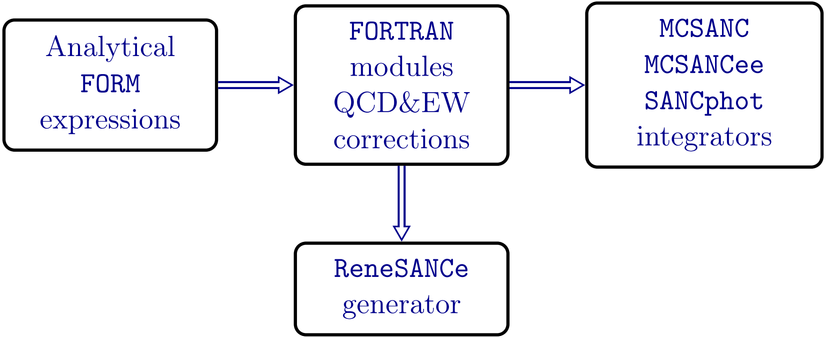

Publications:

SANC – CPC 174 481-517
MCSANC – CPC 184 2343-2350; JETP Letters 103, 131-136
SANCphot – CPC 294 108929
ReneSANCe – CPC 256 107445; CPC 285 108646

SANC products are available at http://sanc.jinr.ru/download.php
ReneSANCe is also available at http://renesance.hepforge.org

SANC advantages:

- **full one-loop electroweak corrections**
- **higher order corrections**
- **massive case**
- **accounting for polarization effects**
- **full phase space operation**
- **results of ReneSANCe event generator and SANC integrators are thoroughly cross checked**

Processes of interest

- Bhabha ($e^+e^- \to e^-e^+$), Phys. Rev. D 98, 013001.
- ZH ($e^+e^- \to ZH$), Phys. Rev. D 100, 073002.
- s-channel ($e^+e^- \to \mu^-\mu^+$, $e^+e^- \to \tau^-\tau^+$), Phys. Rev. D 102, 033004.
- Photon-pair ($e^+e^- \to \gamma\gamma$), Phys. Rev. D 107, 073003.
- s-channel ($e^+e^- \to t\bar{t}$), Phys. Rev. D 107, 113006.
- Muon-electron scattering ($\mu^+e^- \to \mu^+e^-$), Phys. Rev. D 105, 033009.
- Møller ($e^-e^- \to e^-e^-$, $\mu^+\mu^+ \to \mu^+\mu^+$), JETP Lett. 115, 9.
- Zγ ($e^+e^- \to Z\gamma$), JETP Letters 119, 2.
- ZZ ($e^+e^- \to ZZ$), Phys. Rev. D 109, 033012.
- WW ($e^+e^- \to W^+W^-$).

- publication, available in release of the generator
- publication, in preparation for next release of the generator
- in preparation

Basic processes of SM for e^+e^- annihilation

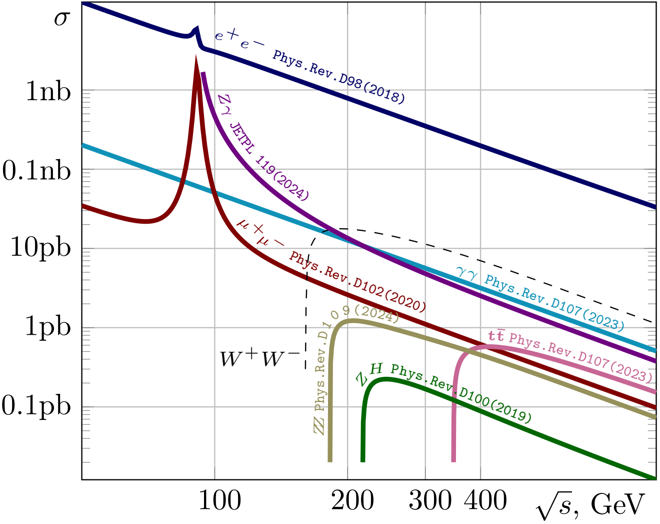

The cross sections are given for polar angles between $10^o < \theta < 170^o$ in the final state.

Distributions

For each process we provide all important distributions:

- Cross section over energy and angle distribution
- Asymmetries: Forward-Backward, Left-Right, ...
- Final-State Fermion Polarization

$e^+e^- \to ZH$, energy dependence

The LO and NLO EW corrected unpolarized cross sections and the relative corrections in parts as a function of the c.m.s. energy.

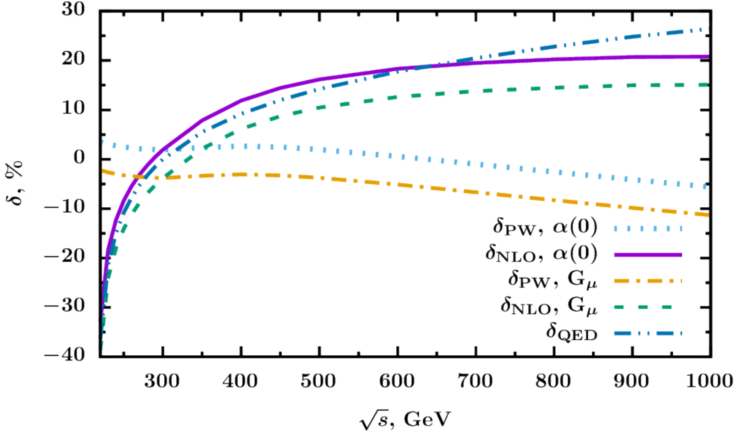

$e^+e^- \to t\bar{t}$, angle dependence

The left part corresponds to the unpolarized (black), and fully polarized, with $(P_{e^+}, P_{e^-} = +1, -1)$ (red) and $(-1, +1)$ (blue), initial beams, while the right one shows the partially polarized initial beams with $(P_{e^+}, P_{e^-} = (+0.3, -0.8)$ (red) and $(-0.3, +0.8)$ (blue) for the energy $\sqrt{s} = 350$ GeV.

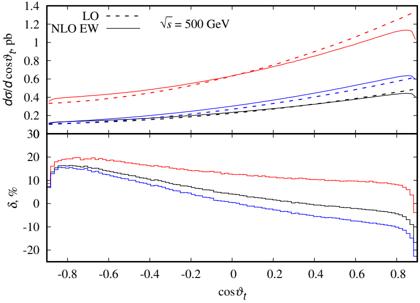

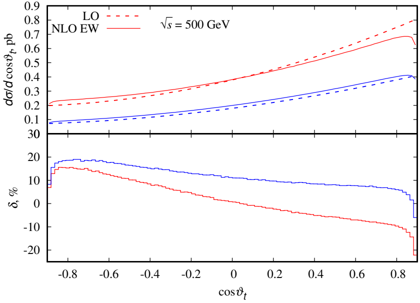

$e^+e^- \to \mu^+\mu^-$, Left–Right Forward–Backward Asymmetry

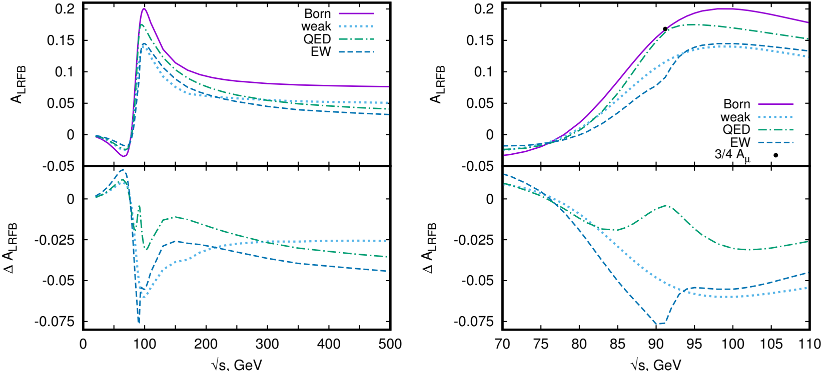

(**Left**) The A_{LRFB} asymmetry in the Born and 1-loop (weak, QED, EW) approximations and ΔA_{LRFB} for c.m.s. energy range; (**Right**) the same for the Z peak region.

$$A_{LRFB} = \frac{(\sigma_{L_e} - \sigma_{R_e})_F - (\sigma_{L_e} - \sigma_{R_e})_B}{(\sigma_{L_e} + \sigma_{R_e})_F + (\sigma_{L_e} + \sigma_{R_e})_B},$$

$e^+e^- \to \tau^+\tau^-$, Final-State Fermion Polarization

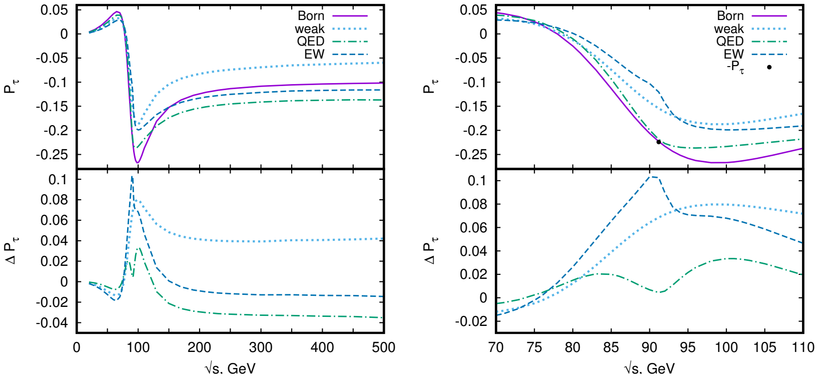

(**Left**) The P_τ polarization in the Born and 1-loop (weak, pure QED, and EW) approximations and ΔP_τ vs. c.m.s. energy in a wide range; (**Right**) the same for the Z peak region. The black dot indicates the value P_τ at the Z resonance.

Hadron-hadron mode

- The following processes are fully implemented in $pp[p\bar{p}]$ mode:
  - $pp[p\bar{p}] \to Z, \gamma \to \ell^+\ell^-$
  - $pp[p\bar{p}] \to W^- \to \ell^-\bar{\nu}_\ell$
  - $pp[p\bar{p}] \to W^+ \to \ell^+\nu_\ell$
- Photon and gluon induced channels can be generated together
- Based on the `SANC` modules
- Complete one-loop and some higher-order electroweak radiative corrections
- Unweighted events in `ROOT` and `LHE` format
- Thoroughly cross checked against `MCSANC` integrator

Polarized DY measurements: motivation

- The measurement of the DY cross section in polarized hadron-hadron collisions would provide important information about the polarization of the quark sea in the nucleon. This measurement and theoretical predictions for polarized DY can be used in PDF fitting programs such as **xFitter**
- The Relativistic Heavy-Ion Collider (RHIC) is the only high-energy spin-polarized proton facility ever built with a working longitudinally polarized mode
- Currently available 93 pb^{-1} of data for longitudinally polarized $p+p$ collisions at $\sqrt{s} = 200$ GeV (from 2009 and 2015 runs by PHENIX and STAR experiments at RHIC) and 569 pb^{-1} at $\sqrt{s} = 510$ GeV (from 2012 and 2013 runs by PHENIX and STAR)
- To increase the accuracy of extracting polarized PDFs, the possibility of collecting an additional 1.1 fb^{-1} at an energy of 510 GeV in 2024-2025 is being considered
- The helicity amplitude (HA) approach can be used for prediction of polarized gauge bosons production at LHC

Polarized PDFs

QUARKS	*unpolarized*	*chiral*	*transverse*
U	f_1		$h_1^{\perp}$
L		g_{1L}	$h_{1L}^{\perp}$
T	$f_{1T}^{\perp}$	g_{1T}	$h_{1T}, h_{1T}^{\perp}$

GLUONS	*unpolarized*	*circular*	*linear*
U	f_1^g		$h_1^{\perp g}$
L		g_{1L}^g	$h_{1L}^{\perp g}$
T	$f_{1T}^{\perp g}$	g_{1T}^g	$h_{1T}^g, h_{1T}^{\perp g}$

- Collinear PDFs: $f_1(x, Q^2)$ (Density), $g_1 \equiv g_{1L}(x, Q^2)$ (Helicity), $h_1(x, Q^2) \equiv h_{1T}(x, Q^2)$ (Transversity)
- TMD PDFs: $f_{1T}^{\perp}(x, Q^2, k_T)$ (Sivers), $g_{1T}^{\perp}(x, Q^2, k_T)$ (Worm-gear-T), $h_{1L}^{\perp}(x, Q^2, k_T)$ (Worm-gear-L), $h_1^{\perp}(x, Q^2, k_T)$ (Boer-Mulders), $h_{1T}^{\perp}(x, Q^2, k_T)$ (Pretzelosity)

Differential cross section

$$d\sigma(\Lambda_1, \Lambda_2, s) = \sum_{q_1 q_2} \sum_{\lambda_1 \lambda_2} \int_0^1 \int_0^1 dx_1 dx_2 f_{q_1}^{\Lambda_1 \lambda_1}(x_1) f_{q_2}^{\Lambda_2 \lambda_2}(x_2) d\hat{\sigma}_{q_1 q_2}(\lambda_1, \lambda_2, \hat{s}),$$

where $\Lambda_i = \pm 1$ and $\lambda_i = \pm 1$ are the helicity of each proton and quark, respectively, with $\hat{s} = x_1 x_2 s$; $f^{\Lambda\lambda} = \frac{1}{2}(f + \Lambda\lambda\Delta f)$.

Observables

We introduce the following combinations of fully polarized components of the hadron-hadron cross section σ^{++}, σ^{+-}, σ^{-+}, σ^{--}:

$$\begin{aligned} \sigma &= \frac{1}{4}\left(\sigma^{++}+\sigma^{+-}+\sigma^{-+}+\sigma^{--}\right)=\sigma^{00}, \\ \Delta\sigma_{\mathrm{L}} &= \frac{1}{4}\left(\sigma^{++}+\sigma^{+-}-\sigma^{-+}-\sigma^{--}\right)=\frac{1}{2}\left(\sigma^{+0}-\sigma^{-0}\right), \\ \Delta\sigma_{\mathrm{LL}} &= \frac{1}{4}\left(\sigma^{++}-\sigma^{+-}-\sigma^{-+}+\sigma^{--}\right). \end{aligned}$$

Single-spin asymmetry is defined by

$$A_{\mathrm{L}}(\mathcal{O})=\frac{d\Delta\sigma_{\mathrm{L}}/d\mathcal{O}}{d\sigma/d\mathcal{O}},$$

and *double-spin* asymmetry is defined by:

$$A_{\mathrm{LL}}(\mathcal{O})=\frac{d\Delta\sigma_{\mathrm{LL}}/d\mathcal{O}}{d\sigma/d\mathcal{O}}$$

for observable $\mathcal{O}$ (we show results for $\mathcal{O}=y_{\mu^+\mu^-},\eta_{\mu^+},\eta_{\mu^-}$).

Neutral Current Drell-Yan: A_L

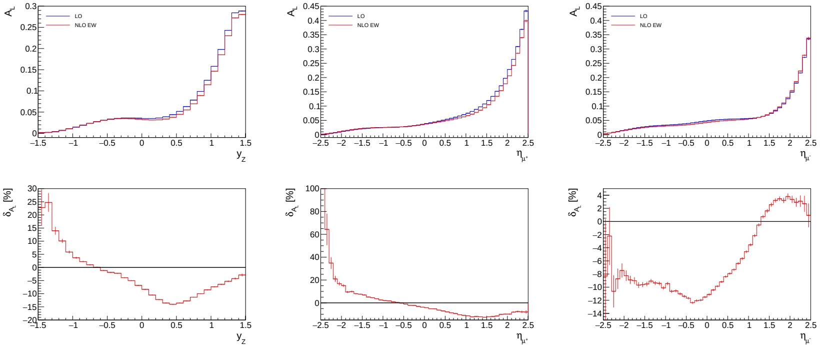

Neutral Current Drell-Yan: A_{LL}

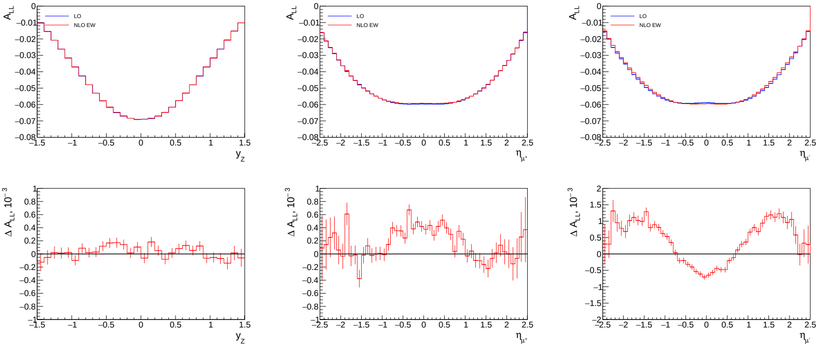

Charged Current Drell-Yan: A_L

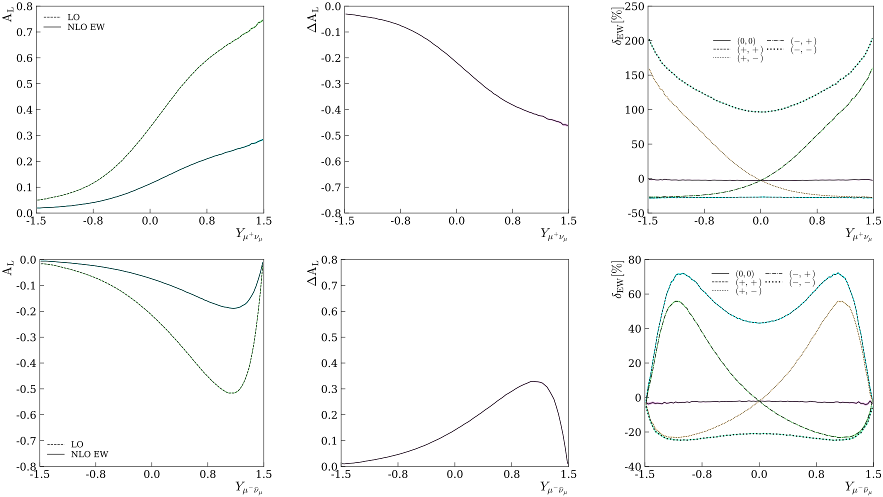

Processes of interest

- $\gamma\gamma \to \gamma\gamma$
- $\gamma\gamma \to Z\gamma$
- $\gamma\gamma \to ZZ$
- $\gamma\gamma \to ZH$
- $\gamma\gamma \to \nu\bar{\nu}$
- $\gamma\gamma \to l^- l^+$
- $\gamma\gamma \to W^- W^+$

First step to transversal polarization.

$\gamma\gamma \to \gamma\gamma$ scattering

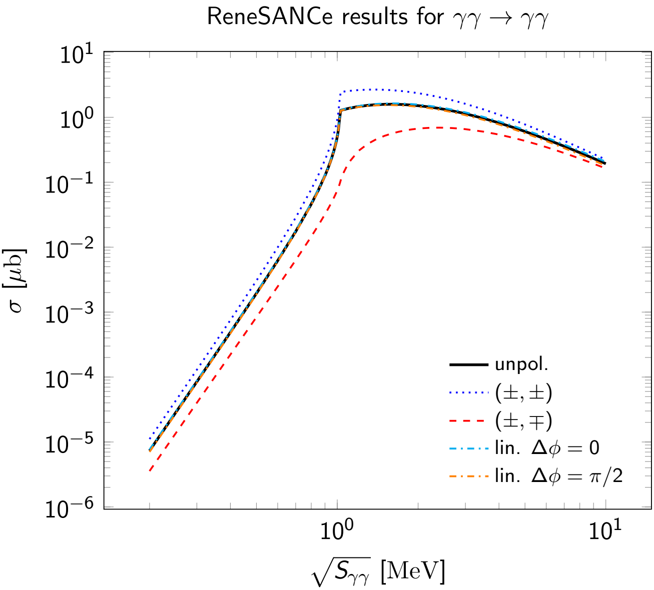

Conclusion

- **Monte Carlo tools of `SANC` provide:**
  - **Complete one-loop EW corrections**
  - **Initial & final state polarization support**
  - **Easy to investigate various asymmetries**
  - **LL-accuracy improvements to cross section**
  - **Higher order improvements throw $\Delta\rho$**
- `ReneSANCe` **provide:**
  - **Events with unit weights**
  - **Output in Standard Les Houches Format**
  - **Simple installation & usage**

- **The research is supported by grant of the Russian Science Foundation (project No. 22-12-00021)**

Backup slides

Higher order improvements

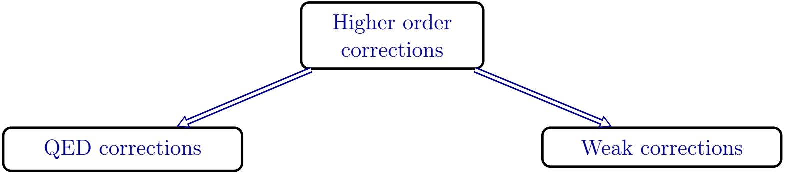

- Leading logarithmic (LL) approximation.
- Corrections to $\Delta\alpha$.
- Shower with matching.

- Corrections to $\Delta\rho$.
- Leading Sudakov logarithms.

Higher order improvements, QED

Basic formula:

$$\sigma^{\mathrm{LLA}} = \int\limits_0^1 \mathrm{d}x_1 \int\limits_0^1 \mathrm{d}x_2 \mathcal{D}_{ee}(x_1)\mathcal{D}_{ee}(x_2)\sigma_0(x_1, x_2, s)\Theta(\mathrm{cuts}),$$

where $\sigma_0(x_1, x_2, s)$ – is the Born level cross section of the annihilation process with changed momenta of initial particles.

$\mathcal{D}_{ee}(x)$ describes the probability density of finding an electron with an energy fraction x in the initial electron beam.

[Kuraev, E.A.; Fadin, V.S. Sov. J. Nucl. Phys. 1985, 41, 466–472]

Higher order improvements, QED

The leading log is $L = \ln \frac{s}{m_l^2}$.

LO	1		
NLO	αL	α	
NNLO	$\frac{1}{2}\alpha^2 L^2$	$\frac{1}{2}\alpha^2 L$	$\frac{1}{2}\alpha^2$
$\mathrm{N^3LO}$	$\frac{1}{6}\alpha^3 L^3$	$\frac{1}{6}\alpha^3 L^2$	$\ldots$

In the LL approximation we can separate pure photonic (marked "γ") and the rest corrections which include pure pair and mixed photon-pair effects (marked as "pair").

$e^+e^- \to t\bar{t}$, $\sqrt{s}$ =350 and 500 GeV

Multiple photon ISR relative corrections δ (%) in the LLA approximation.

$\sqrt{s}$, GeV	350	500
$\mathcal{O}(\alpha L)$, γ	$-42.546(1)$	$-3.927(1)$
$\mathcal{O}(\alpha^2 L^2)$, γ	$+8.397(1)$	$-0.429(1)$
$\mathcal{O}(\alpha^2 L^2)$, e^+e^-	$-0.460(1)$	$-0.030(1)$
$\mathcal{O}(\alpha^2 L^2)$, $\mu^+\mu^-$	$-0.277(1)$	$-0.018(1)$
$\mathcal{O}(\alpha^3 L^3)$, γ	$-0.984(1)$	$+0.021(1)$
$\mathcal{O}(\alpha^3 L^3)$, e^+e^-	$+0.182(1)$	$-0.012(1)$
$\mathcal{O}(\alpha^3 L^3)$, $\mu^+\mu^-$	$+0.110(1)$	$-0.008(1)$
$\mathcal{O}(\alpha^4 L^4)$, γ	$+0.070(1)$	$+0.002(1)$

Higher order improvements, weak

Higher order improvements added to NLO cross section through $\Delta\rho$ parameter: $s_W^2 \rightarrow \bar{s}_W^2 \equiv s_W^2 + \Delta\rho\, c_W^2$.

$\mathcal{O}(\alpha)$	A. Sirlin, PRD22, (1980) 971, W.J. Marciano, A. Sirlin, PRD22 (1980) 2695; G. Degrassi, A. Sirlin, NPB352 (1991) 352, P. Gambino and A. Sirlin, PRD49 (1994) 1160
$\mathcal{O}(\alpha\alpha_s)$	A. Djouadi, C. Verzegnassi, PLB195 (1987) 265; B. Kiehl, NPB353 (1991) 567; B. Kniehl, A. Sirlin, NPB371 (1992) 141, PRD47 (1993) 883; A. Djouadi, P. Gambino, PRD49 (1994) 3499
$\mathcal{O}(\alpha\alpha_s^2)$	L. Avdeev et al., PLB336 (1994) 560;K.G. Chetyrkin, J.H. Kuhn, M. Steinhauser, PLB351 (1995) 331; PRL75 (1995) 3394; NPB482 (1996)
$\mathcal{O}(\alpha\alpha_s^3)$	Y. Schroder, M. Steinhauser, PLB622 (2005) 124; K.G. Chetyrkin et al., hep-ph/0605201; R. Boughezal, M. Czakon, hep-ph/0606232
$\mathcal{O}(\alpha^2)$	G. Degrassi, P. Gambino, A. Sirlin, PLB394 (1997) 188; M. Awramik, M. Czakon, A. Freitas, JHEP0611 (2006) 048

$e^+e^- \to t\bar{t}$, $\sqrt{s}$ =350 and 500 GeV

Integrated Born and weak contributions to the cross section and higher-order leading corrections in two EW schemes: $\alpha(0)$ and G_μ.

$\sqrt{s}$, GeV	350	500
$\sigma^{\text{Born}}_{\alpha(0)}$, pb	0.22431(1)	0.45030(1)
$\sigma^{\text{Born}}_{G_\mu}$, pb	0.24108(1)	0.48398(1)
$\delta^{\text{Born}}_{G_\mu/\alpha(0)}$, %	7.48(1)	7.48(1)
$\sigma^{\text{weak}}_{\alpha(0)}$, pb	0.25564(1)	0.47705(1)
$\sigma^{\text{weak}}_{G_\mu}$, pb	0.26055(1)	0.48420(1)
$\delta^{\text{weak}}_{G_\mu/\alpha(0)}$, %	1.92(1)	1.50(1)
$\sigma^{\text{weak+ho}}_{\alpha(0)}$, pb	0.25900(1)	0.48483(1)
$\sigma^{\text{weak+ho}}_{G_\mu}$, pb	0.25986(1)	0.48289(1)
$\delta^{\text{weak+ho}}_{G_\mu/\alpha(0)}$, %	0.33(1)	−0.40(1)